

# Theoretical Studies of the Electrocyclic Reaction Mechanisms of *o*-Xylylene to Benzocyclobutene

Shogo Sakai

Department of Information Systems Engineering, Faculty of Engineering, Osaka Sangyo University, Daito 574-8530, Japan

Received: July 5, 2000; In Final Form: September 13, 2000

The potential energy surfaces for the electrocyclic reactions of *o*-xylylene to benzocyclobutene were calculated by ab initio molecular orbital methods. The transition states of two reaction pathways, conrotatory and disrotatory, for the electrocyclic reaction of *o*-xylylene were obtained. The difference of energy barriers on the conrotatory and the disrotatory pathways is extremely low: 7.4 kcal/mol as determined by complete active space self-consistent field (CASSCF) calculations and 8.0 kcal/mol as determined by complete active space second-order Møller-Plesset perturbation (CAS-MP2) calculations. The energy difference due to the orbital phase such as the orbital symmetry rules was also estimated: 3.5 kcal/mol at the CAS-MP2 calculations. These mechanisms along the conrotatory and the disrotatory reaction pathways were analyzed by the configuration interaction (CI)-localized molecular orbital (LMO)-CASSCF along the intrinsic coordinate (IRC) pathway (CiLC-IRC) method.

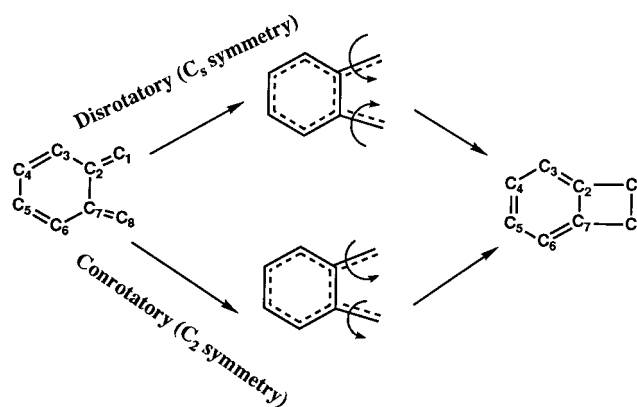
## 1. Introduction

Pericyclic reactions are the most important organic reactions. The mechanisms of these reactions have been the subject of the most heated and interesting controversies.<sup>1,2</sup> The orbital symmetry rules, such as the Woodward-Hoffmann rule<sup>3</sup> and the frontier orbital theory,<sup>4</sup> defined the concept of a pericyclic reaction. The rules served not to settle mechanistic questions but to raise the stakes on what were already lively controversies.

In our previous papers, the electrocyclic reaction mechanisms for butadiene,<sup>5</sup> disilylbutadiene,<sup>5</sup> and hexatriene<sup>6</sup> were reported. Analysis of these reaction paths by a configuration interaction (CI)-localized molecular orbital (LMO)-complete active space self-consistent field (CASSCF) calculation along the intrinsic reaction coordinate (IRC) pathway (CI-LMO-CAS//IRC; CiLC-IRC) indicates that the difference between the conrotatory and the disrotatory mechanisms is explained by the biradical character of the terminal atoms. For the transition states on the conrotatory and the disrotatory pathways, the energy difference of both transition states was estimated for butadiene (19.5 kcal/mol), 1,4-disilylbutadiene (4.2 kcal/mol), and hexatriene (10.4 kcal/mol). The energy differences due to the orbital phase for butadiene and 1,4-disilylbutadiene were 10.6 and 3.4 kcal/mol, respectively. For the electrocyclic reaction of *o*-xylylene, the comparison of the conrotatory and the disrotatory mechanisms to be regarded formally as either a  $4\pi$ - or an  $8\pi$ -electron process is interesting in the characterization of a electrocyclic reaction.

It is known<sup>7</sup> that the electrocyclic reaction for *o*-xylylene occurs through the conrotatory path ( $C_2$  symmetry) for thermal excitation and not through the disrotatory path ( $C_s$  symmetry).

Houk and co-workers<sup>7</sup> have calculated the transition state geometry on the conrotatory reaction pathway for the electrocyclic isomerization of *o*-xylylene to benzocyclobutene by ab initio MO methods. They pointed out that the activation energy for the ring closure is 40 kcal/mol at the HF/3-21G calculation level. However, the disrotatory reaction path and the difference of energy barrier heights between the conrotatory and the disrotatory pathways are, to our knowledge, unknown.



In this paper, we report the potential energy surfaces for the conrotatory and the disrotatory pathways of electrocyclic reactions of *o*-xylylene at the CASSCF MO calculation level. These electrocyclic reaction pathways are also analyzed by CiLC-IRC methods.

## 2. Methods of Computation

All equilibrium and transition state geometries for electrocyclic reactions of *o*-xylylene to benzocyclobutene were determined with analytically calculated energy gradients by the CASSCF method<sup>8</sup> with the 6-31G(d,p) basis set.<sup>9,10</sup> For the CASSCF calculation, eight active spaces corresponding to four  $\pi$  and  $\pi^*$  orbitals for *o*-xylylene and related systems were included. All configurations in active spaces were generated. Single-point energies were determined at a multiconfigurational second-order Møller-Plesset perturbation (CAS-MP2)<sup>11</sup> with the 6-311+G(d,p) basis set<sup>12</sup> using the CASSCF-optimized structures. The IRC<sup>13,14</sup> was followed from the transition state toward both reactants and products.

To interpret the mechanisms along the reaction pathways, a CiLC-IRC analysis with the 6-31G(d,p) basis set was carried out with the following method that has been described elsewhere:

<sup>5,6,15–19</sup> (1) The CASSCF is calculated to obtain a starting set of orbitals for the localization procedure. (2) After the CASSCF procedure is carried out, the eight CASSCF-optimized orbitals are localized by the Boys localization procedure.<sup>20</sup> The localized orbitals are atomic in nature. (3) Using the localized MOs as a basis, a full CI at the Slater determinants level is used to generate electronic structures and their relative weights in the atomic orbital-like wave functions. The calculated total energy by the CI method in the process corresponds to that determined by the CASSCF calculation. The calculation procedures are repeated along the IRC pathway, which we call a CiLC–IRC analysis for the procedures. From the analysis of the results, we can see the change of electronic state on the basis of atomic-like orbitals. The CiLC method is used as a kind of valence bond explanation<sup>21–23</sup> of the CASSCF wave function.

The CiLC–IRC calculations were performed with the GAMESS program package.<sup>24</sup> The other calculations were carried out with the Gaussian98 program.<sup>25</sup>

### 3. Results and Discussion

**3.1 Reaction Pathways.** The optimized geometries of *o*-xylylene, the conrotatory transition state, the disrotatory transition state, and benzocyclobutene are shown in Figure 1. In Figure 1, to compare with the cyclic reactions of butadiene, the corresponding geometry parameters of butadiene systems are in given in parentheses. The total energies and the relative energies are listed in Table 1.

The optimized geometry of *o*-xylylene is a planar at the CAS-(8,8)/6-31G(d,p) calculation. The geometry of *o*-xylylene calculated by the HF/6-31G(d,p) and density function (B3LYP/6-31G(d,p)) methods indicate a nonplanar structure with a  $C_2$  symmetry. The dihedral angle of  $C_1-C_2-C_7-C_8$  is  $21.8^\circ$  and  $15.5^\circ$  degree as determined by the HF/6-31G(d,p) and the B3LYP/6-31G(d,p) methods, respectively. The energy difference between the planar and nonplanar geometries is only 0.3 and 0.1 kcal/mol as determined by the HF/6-31G(d,p) and the B3LYP/6-31G(d,p) methods, respectively. The experimental observation<sup>26–31</sup> from the strong fluorescence characteristic of *o*-xylylene suggests nearly planar geometry and corresponds to the results of our CASSCF calculation. The geometrical variation of planar and nonplanar is loose because the twisting mode corresponding to the dihedral angle of  $C_1-C_2-C_7-C_8$  is very small ( $20\text{ cm}^{-1}$ ) according to the CAS(8,8)/6-31G(d,p) calculation. The bond alternation of C–C and C=C as a Kekulé structure for the geometry of the calculated *o*-xylylene is seen, which is quite marked.

For the conrotatory transition state, the dihedral angle of  $C_1-C_2-C_7-C_8$  is  $17.5^\circ$ , which corresponds to that ( $18.8^\circ$  degree) of the conrotatory transition state for the cyclization of butadiene.<sup>5</sup> Although the bond length of  $C_2-C_7$  of *o*-xylylene is 0.13 Å longer than that of  $C_1-C_2$  (or  $C_7-C_8$ ), the bond length of  $C_2-C_7$  of the transition state is 0.06 Å shorter than that of  $C_1-C_2$  (or  $C_7-C_8$ ). Accordingly, from the comparison of the bond lengths of  $C_2-C_7$  and  $C_1-C_2$  (or  $C_7-C_8$ ), the transition state is “a late transition state”. We will discuss the late transition state in the following section. The activation energy calculated by the CAS-MP2 method for the cyclization of *o*-xylylene is 34.9 kcal/mol, which is 5 kcal/mol smaller than the experimental value (39.9 kcal/mol).<sup>32–34</sup> The heat of reaction for the cyclization reaction of *o*-xylylene is exothermic by 8 kcal/mol, which is also 5 kcal/mol smaller than the experimental values (13 kcal/mol).<sup>32–34</sup> Comparing the conrotatory cyclic reaction of *o*-xylylene with that of butadiene, the activation energy for the reaction of *o*-xylylene is about 14 kcal/mol lower

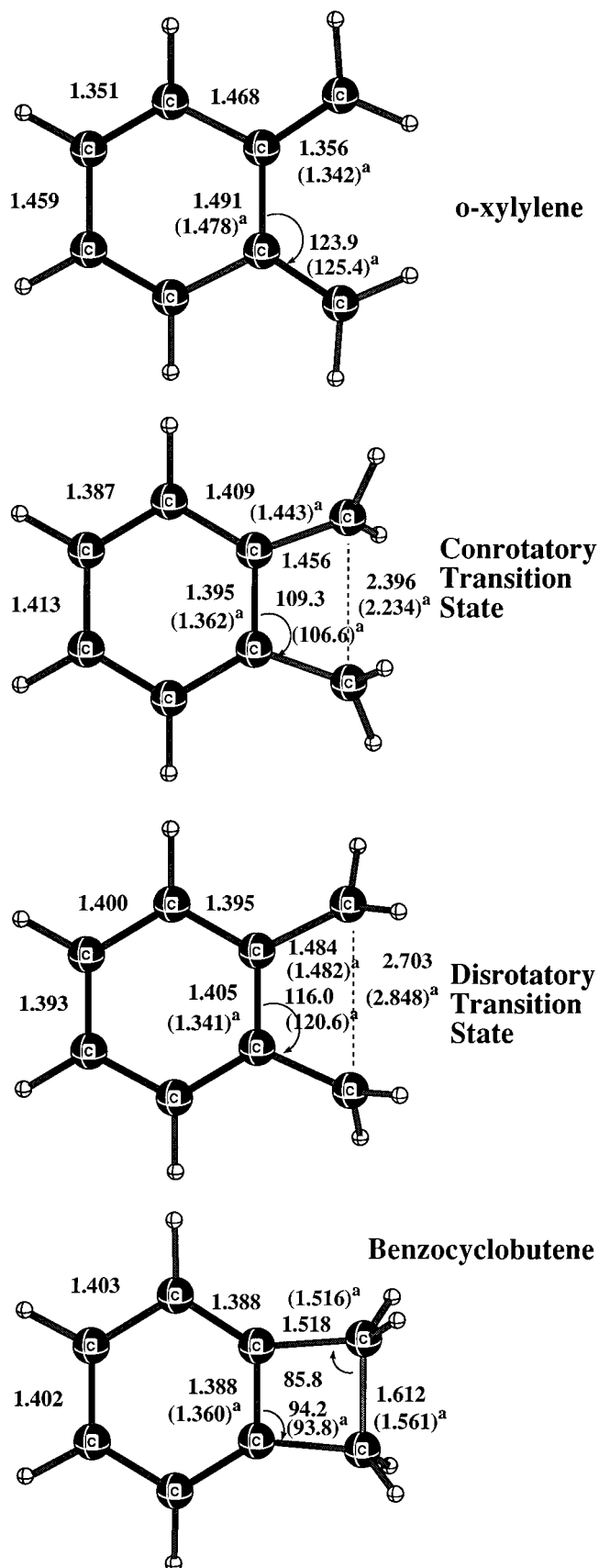


**Figure 1.** Stationary point geometries (in Å and degrees) for electrocyclic reaction of *o*-xylylene at the CAS/6-31G(d,p) level. (a) The corresponding geometry parameters of butadiene systems are in given in parentheses.

than that of butadiene at the CAS-MP2 calculation level. This energy difference may come from the aromatic energy of the

**TABLE 1: Total Energies (Hartree) and Relative Energies (kcal/mol) for the Electrocyclic Reactions of *o*-Xylylene and the Corresponding Relative Energies for Electrocyclic Reaction of *cis*-Butadiene<sup>a</sup>**

compound	CAS/6-31G(d,p)	CAS-MP2/6-31G(d,p)	CAS/6-311+G(d,p)	CAS-MP2/6-311+G(d,p)	Exp <sup>b</sup>
<i>o</i> -Xylylene	-307.66678 (0.0)	-308.58198 (0.0)	-307.72177 (0.0)	-308.79569 (0.0)	(0.0)
Conrotatory TS	-307.60814 (36.8)	-308.52614 (35.0)	-307.66259 (37.1)	-308.74003 (34.9)	(26.9)
Disrotatory TS	-307.59651 (44.1)	-308.51327 (43.1)	-307.65091 (44.5)	-308.72732 (42.9)	
Benzocyclobutene	-307.66966 (-1.8)	-308.59625 (-9.0)	-307.72218 (-0.3)	-308.80836 (-8.0)	(-13)
<i>cis</i> -butadiene <sup>c</sup>		(0.0)		(0.0)	
Conrotatory TS <sup>c</sup>		(49.3)		(49.0)	
Disrotatory TS <sup>c</sup>		(68.6)		(68.5)	
Cyclobutene <sup>c</sup>		(9.2)		(9.9)	

<sup>a</sup> The relative energies are given in parentheses. <sup>b</sup> Experimental observation of refs 32–34. <sup>c</sup> Reference 5.

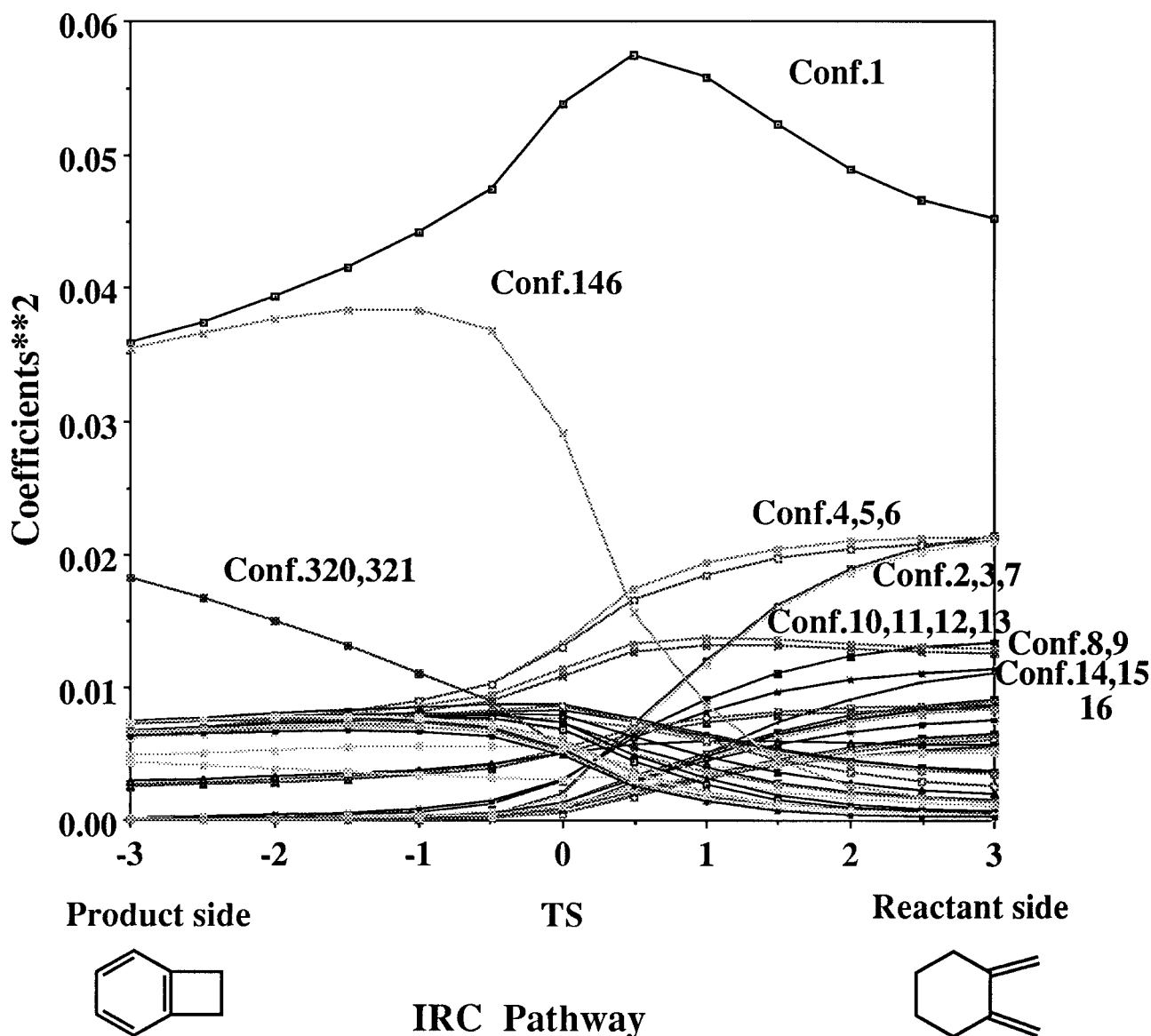


**Figure 2.** Square of CI coefficients by the CiLC-IRC along the conrotatory pathway for electrocyclic reaction of *o*-xylylene. The unit of IRC is bohr amu<sup>1/2</sup>.

benzene part because the largest difference in all C–C bond lengths of the benzene-ring part of *o*-xylylene is 0.14 Å between C<sub>2</sub>–C<sub>7</sub> and C<sub>3</sub>–C<sub>4</sub> (or C<sub>5</sub>–C<sub>6</sub>) bonds. For the conrotatory transition state, this difference is 0.026 Å between C<sub>4</sub>–C<sub>5</sub> and C<sub>3</sub>–C<sub>4</sub> (or C<sub>5</sub>–C<sub>6</sub>) bonds. Therefore, the benzene ring part of *o*-xylylene corresponds to a Kekulé structure and that of the conrotatory transition state may be an aromatic structure.

For the disrotatory pathway, the transition state has two negative eigenvalues for the force-constant-matrix determined by the CAS/6-31G(d,p) method. The eigenvector of one negative eigenvalue corresponds to the reaction coordinate with a' symmetry. The other eigenvalue is 202 cm<sup>-1</sup> with a'' symmetry as determined by the CAS/6-31G(d,p) method. The a'' negative eigenvalue is directed toward each of the two conrotatory

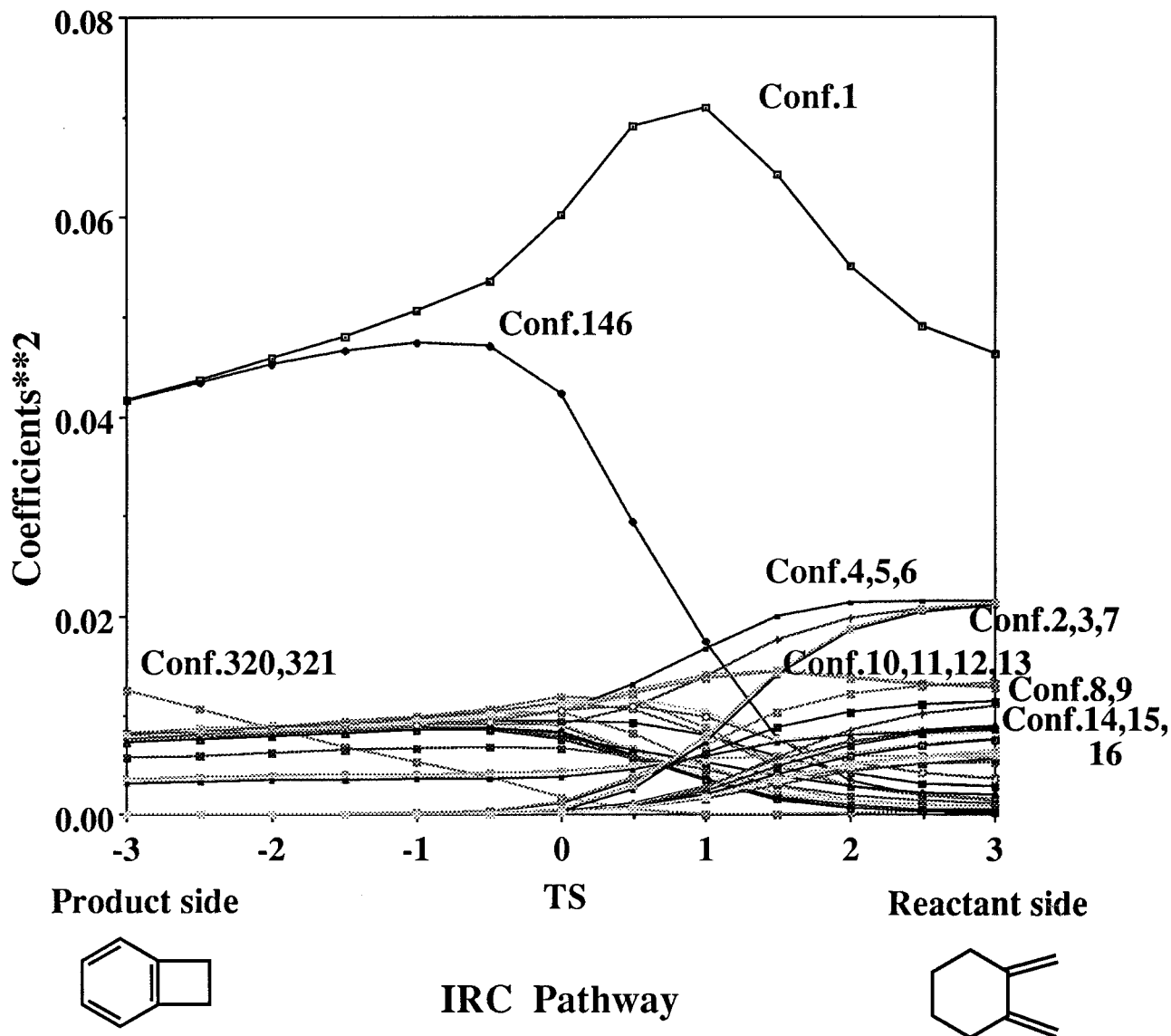


**Figure 3.** Square of CI coefficients by the CiLC-IRC along the disrotatory pathway for electrocyclic reaction of *o*-xylylene. The unit of IRC is bohr amu<sup>1/2</sup>.

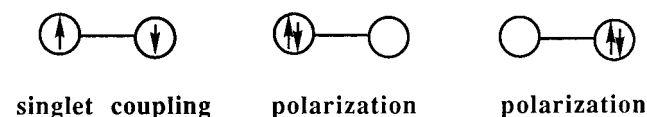
transition states corresponding to the two alternatives of clockwise and counterclockwise rotation of the CH<sub>2</sub> groups. The disrotatory double-saddle point is therefore a hill in the broader valley of the potential energy surface formed by the two equivalent conrotatory transition states. Consequently, the transition state on the disrotatory pathway is not a real transition state as is the disrotatory transition state for cyclization of butadiene. The energy difference between the conrotatory and the disrotatory transition state is only 7.4 kcal/mol as determined by the CASSCF method and 8.0 kcal/mol according to the CAS-MP2 calculations. The energy differences are very small in comparison with those for cyclization of butadiene: 13.3 kcal/mol according to the CASSCF calculation and 19.6 kcal/mol according to the CAS-MP2 calculations. This small difference comes from the benzene ring because the C-C bond distances of benzene ring for the disrotatory transition state are almost the same lengths. In fact, the largest differences in the all C-C bond lengths of the benzene ring are 0.012 Å for the disrotatory transition state and 0.026 Å for the conrotatory transition state. Therefore, for the disrotatory transition state, the six-membered ring stabilizes with aromatic energy because the terminal carbon atoms have a bi-radical nature, as shown in the previous paper,<sup>5</sup> for the cyclic reaction of butadiene.

The orbital symmetry rule characterizes the reactions of the conrotatory and the disrotatory pathways as allowed and forbidden reactions with the orbital phase. On the other hand, the calculated two transition states have different dihedral angles of the C<sub>1</sub>-C<sub>2</sub>-C<sub>7</sub>-C<sub>8</sub>: 17.5° for the conrotatory and 0.0° for the disrotatory. Thus, the difference of the activation energies for the conrotatory and disrotatory pathways includes not only the effects of the orbital phase but also the geometry effects. To obtain the difference of energy barriers due to the orbital phase for both reaction pathways, the transition state of the conrotatory type with the restriction of dihedral angle (C<sub>1</sub>-C<sub>2</sub>-C<sub>7</sub>-C<sub>8</sub>) of 0.0° was also calculated at the CAS/6-31G(d,p) level. The two carbon atoms (C<sub>3</sub> and C<sub>6</sub>) bonding to C<sub>2</sub> and C<sub>7</sub> atoms were also located in the C<sub>1</sub>-C<sub>2</sub>-C<sub>7</sub>-C<sub>8</sub> plane. The energy barrier height of the restricted transition state is 40.0 kcal/mol above the reactant (*o*-xylylene) at the CAS/6-31G(d,p) level, and the difference of the energy barriers between the restricted transition state of the conrotatory type and the transition state of the disrotatory type is 4.1 kcal/mol at the CAS/6-31G(d,p) level. According to our best calculation, CAS-MP2/6-311+G(d,p), the difference of the energy barriers is 3.5 kcal/mol. Therefore, about half of the energy difference of the transition states on the conrotatory and disrotatory pathways

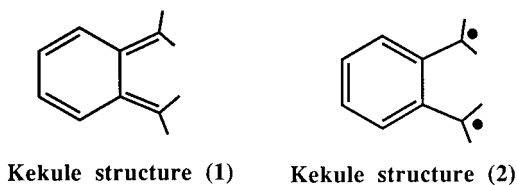
comes from the orbital phase and the other half of the energy comes from the geometrical effects.<sup>35</sup> The relation of the orbital phase and the geometrical effects is the same as that of the cyclic reaction of butadiene; namely, for the cyclic reaction of butadiene, the difference (19.5 kcal/mol) of the energy barriers between the transition states of the conrotatory and the disrotatory pathways includes about half (10.6 kcal/mol) of them from the orbital phase effects.

For benzocyclobutene, all C–C bond lengths of the six-membered ring are almost the same lengths. The largest difference in these bond lengths is only 0.015 Å between C<sub>2</sub>–C<sub>3</sub> (or C<sub>2</sub>–C<sub>7</sub>, C<sub>6</sub>–C<sub>7</sub>) and C<sub>3</sub>–C<sub>4</sub> bonds. Accordingly, the six-membered ring part may be aromatic benzene.

**3.2 CiLC–IRC Analysis.** To study the electronic mechanisms on the conrotatory and disrotatory pathways for the cyclic reactions of *o*-xylylene, the CiLC–IRC analysis was performed. The weights of CI coefficients by the CiLC–IRC method for the conrotatory and disrotatory pathways are displayed in Figures 2 and 3. In these figures, the reactant side (*o*-xylylene) of the IRC corresponds with positive values of the coordinate and the product side (benzocyclobutene) corresponds with negative values. The configurations with the small values (<0.005) for the maximum weight of each configuration were neglected in Figures 2 and 3. Some configurations for the large weights of CI coefficients in Figures 2 and 3 are shown in Figure 4. For the reactant side, *o*-xylylene, in Figure 2 or 3, the configurations 2, 3, 4, and 5, could be described as the singlet coupling terms of C<sub>7</sub>–C<sub>8</sub>, C<sub>1</sub>–C<sub>2</sub>, C<sub>5</sub>–C<sub>6</sub>, and C<sub>3</sub>–C<sub>4</sub> bonds, respectively. The sets of two configurations of 8 and 14, 9 and 15, 11 and 12, and 10 and 13 could be described as the polarization terms for C<sub>7</sub>–C<sub>8</sub>, C<sub>1</sub>–C<sub>2</sub>, C<sub>5</sub>–C<sub>6</sub>, and C<sub>3</sub>–C<sub>4</sub> bonds, respectively. Therefore, the sets of the configurations of {2,8,14}, {3,9,15}, {4,11,12}, and {5,10,13} can be described as the  $\pi$  bonds of C<sub>7</sub>–C<sub>8</sub>, C<sub>1</sub>–C<sub>2</sub>, C<sub>5</sub>–C<sub>6</sub>, and C<sub>3</sub>–C<sub>4</sub>, respectively. In fact, the  $\pi$  bonding of ethylene can be described as the singlet coupling between p $_{\pi}$  orbitals plus two polarization terms, as shown next.



The configurations 6 and 7 mean that the electronic state of *o*-xylylene is not the coupling of two butadiene types as C<sub>3</sub>–C<sub>4</sub>–C<sub>5</sub>–C<sub>6</sub> and C<sub>1</sub>–C<sub>2</sub>–C<sub>7</sub>–C<sub>8</sub> or C<sub>1</sub>–C<sub>2</sub>–C<sub>3</sub>–C<sub>4</sub> and C<sub>5</sub>–C<sub>6</sub>–C<sub>7</sub>–C<sub>8</sub>. The configuration 6 also means the separation for four bonds of C<sub>1</sub>–C<sub>2</sub>, C<sub>3</sub>–C<sub>4</sub>, C<sub>5</sub>–C<sub>6</sub>, and C<sub>7</sub>–C<sub>8</sub>. The weights of the other configurations are smaller than those of the aforementioned configurations. Therefore, *o*-xylylene is a typical Kekulé structure (1). The weights of the configuration of Kekulé structure (2) are very small. Accordingly, the six-membered ring



of *o*-xylylene does not have aromatic nature, which corresponds to the bond alternation of six-membered ring for the geometry in Figure 1.

On the other hand, for the benzocyclobutene product side, the configuration 146 could be described as the singlet coupling

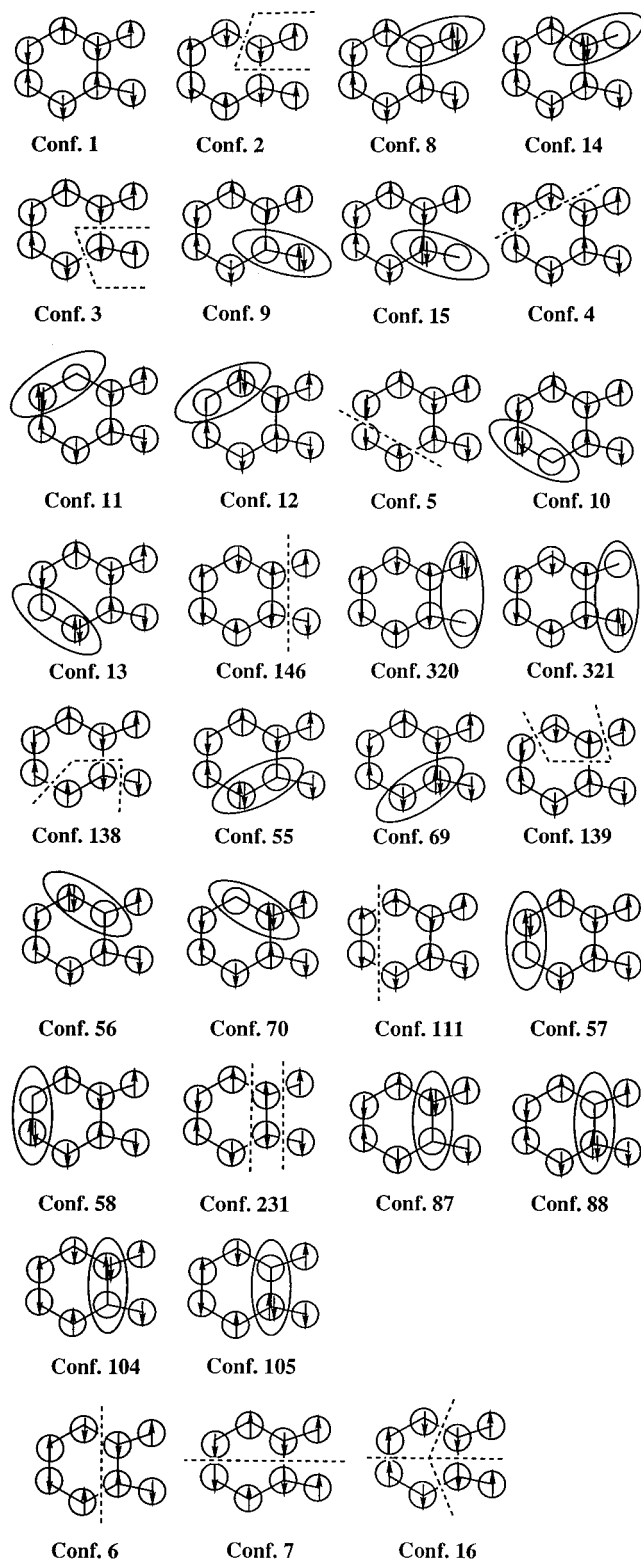


**Figure 4.** Some electronic configurations of the electrocyclic reactions of *o*-xylylene for CiLC–IRC analysis.

term of C<sub>1</sub>–C<sub>8</sub>. The configurations 320 and 321 could be described as the polarization terms of C<sub>1</sub>–C<sub>8</sub>. Therefore, the configuration set of {146,320,321} can be described as the  $\sigma$  bond of C<sub>1</sub>–C<sub>8</sub>. In the same way as for the aforementioned configurations of *o*-xylylene, the configuration sets of {138,55,69}, {139,56,70}, and {111,57,58} indicate the  $\pi$  bonds of C<sub>2</sub>–C<sub>3</sub>, C<sub>6</sub>–C<sub>7</sub>, and C<sub>4</sub>–C<sub>5</sub>, respectively. For the benzocyclobutene product side, the weights of the six configuration sets {2,8,14}, {3,9,15}, {4,11,12}, {5,10,13}, {138,55,69}, {139,-

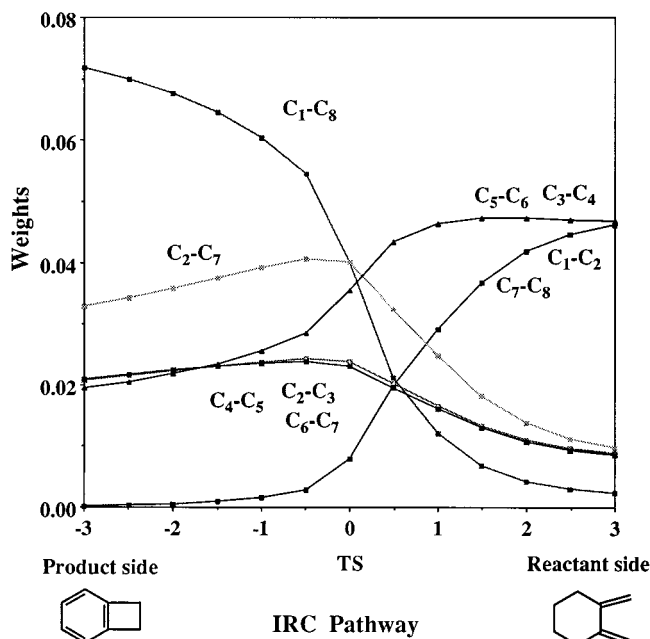


**Figure 5.** Sum of the weights of CI coefficients of the singlet coupling and polarization terms of the CiLC-IRC along the conrotatory pathway for the electrocyclic reaction of *o*-xylylene. The unit of IRC is bohr  $\text{amu}^{1/2}$ .

56,70}, and {111,57,58} show almost the same values. The weights of other higher excited configurations for the six-membered ring are small at the product side. Therefore, the six-membered ring of benzocyclobutene is described as the configuration sets of six  $\pi$  bonds of C<sub>2</sub>-C<sub>3</sub>, C<sub>3</sub>-C<sub>4</sub>, C<sub>4</sub>-C<sub>5</sub>, C<sub>5</sub>-C<sub>6</sub>, C<sub>6</sub>-C<sub>7</sub>, and C<sub>7</sub>-C<sub>2</sub>. This description is the same in case of the aromatic structure that was shown in the previous paper<sup>18,19</sup> that compared the Kekulé structure with the aromatic structure for benzene.

For the conrotatory pathway with C<sub>2</sub> symmetry in Figure 2, the crossing between the singlet coupling terms of C<sub>1</sub>-C<sub>2</sub> (or C<sub>7</sub>-C<sub>8</sub>) and C<sub>1</sub>-C<sub>8</sub> occurs at the reactant side of  $\sim 0.8$  bohr  $\text{amu}^{1/2}$  on the IRC pathway. The crossing between the polarization terms of C<sub>1</sub>-C<sub>2</sub> (or C<sub>7</sub>-C<sub>8</sub>) and C<sub>1</sub>-C<sub>8</sub> also occurs at the reactant side of 0.2–0.5 bohr  $\text{amu}^{1/2}$ . Therefore, the bond exchange of the old  $\pi$  bonds of C<sub>1</sub>-C<sub>2</sub> (and C<sub>7</sub>-C<sub>8</sub>) and the new  $\sigma$  bond of C<sub>1</sub>-C<sub>8</sub> occurs before the transition state, which corresponds to the “late transition state” described in the previous section. The weights of the configuration sets of {4,-11,12} and {5,10,13} decrease drastically in the region between 0.5 and  $-0.5$  bohr  $\text{amu}^{1/2}$  on the IRC pathway. Therefore, the  $\pi$  bonds of C<sub>3</sub>-C<sub>4</sub> and C<sub>5</sub>-C<sub>6</sub> are weak in the vicinity of the transition state. To the contrary, the weights of the configuration sets of C<sub>2</sub>-C<sub>3</sub>, C<sub>4</sub>-C<sub>5</sub>, C<sub>6</sub>-C<sub>7</sub>, and C<sub>2</sub>-C<sub>7</sub> of the benzene ring increase in the vicinity of the transition state. To make more clear a scheme of mechanisms just presented, the sums for the weights of the CI coefficients of the singlet coupling and polarization terms for each bonds along the conrotatory pathway are displayed in Figure 5. As seen in Figure 5, the crossing between the bonds of C<sub>1</sub>-C<sub>8</sub> and C<sub>1</sub>-C<sub>2</sub> (or C<sub>7</sub>-C<sub>8</sub>) occurs at  $\sim 0.5$  bohr  $\text{amu}^{1/2}$ . At the transition state on the conrotatory pathway, the weights of the bonds of C<sub>3</sub>-C<sub>4</sub> and C<sub>5</sub>-C<sub>6</sub> are still larger than those of the bonds of C<sub>2</sub>-C<sub>3</sub>, C<sub>4</sub>-C<sub>5</sub>, and C<sub>6</sub>-C<sub>7</sub>. Consequently, the six membered ring of the conrotatory transition state is not the complete aromatic structure.

For the disrotatory pathway with C<sub>s</sub> symmetry, as shown in Figure 3, the crossing between the singlet coupling terms of C<sub>1</sub>-C<sub>2</sub> (or C<sub>7</sub>-C<sub>8</sub>) and C<sub>1</sub>-C<sub>8</sub> occurs also at the reactant side

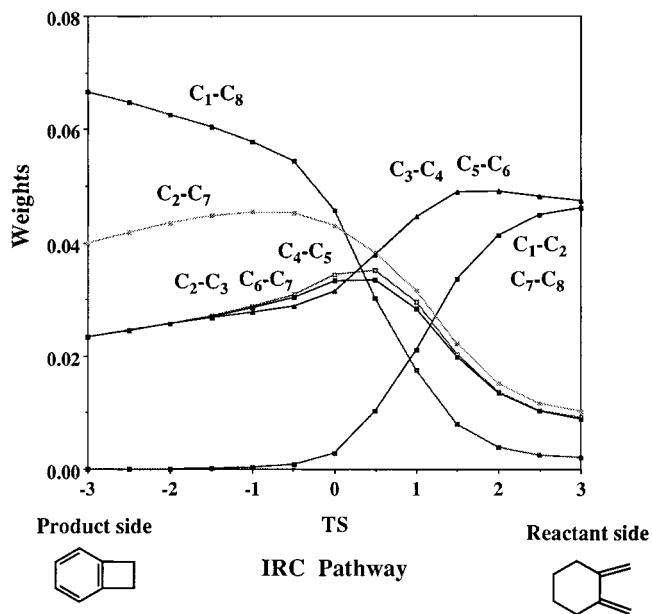


**Figure 6.** Sum of the weights of CI coefficients of the singlet coupling and polarization terms of the CiLC-IRC along the disrotatory pathway for the electrocyclic reaction of *o*-xylylene. The unit of IRC is bohr  $\text{amu}^{1/2}$ .

of  $\sim 1.3$  bohr  $\text{amu}^{1/2}$  on the IRC pathway. The crossing between the polarization terms of C<sub>1</sub>-C<sub>2</sub> (or C<sub>7</sub>-C<sub>8</sub>) and C<sub>1</sub>-C<sub>8</sub> occurs in the vicinity of  $\sim 0.5$  bohr  $\text{amu}^{1/2}$  on the IRC pathway. The weights of these polarization terms are almost zero at the crossing points. This result means that the reaction occurs through the bi-radical character at the C<sub>1</sub> and C<sub>8</sub> atoms in the vicinity of 0.5 bohr  $\text{amu}^{1/2}$  on the IRC pathway. The bi-radical character at the terminal atoms is similar to that of the disrotatory reaction of butadiene. To make more simple the scheme of the mechanisms, the sums for the weights of the CI coefficients of single coupling and polarization terms for each bonds along the disrotatory pathway are shown in Figure 6. As seen in Figure 6, the crossing between the bonds of C<sub>1</sub>-C<sub>8</sub> and C<sub>1</sub>-C<sub>2</sub> (or C<sub>7</sub>-C<sub>8</sub>) occurs at  $\sim 0.9$  bohr  $\text{amu}^{1/2}$ , and this crossing point is earlier than that of the conrotatory pathway. At the transition state on the disrotatory pathway, the weights of the C<sub>3</sub>-C<sub>4</sub>, C<sub>5</sub>-C<sub>6</sub>, C<sub>2</sub>-C<sub>3</sub>, C<sub>4</sub>-C<sub>5</sub>, and C<sub>6</sub>-C<sub>7</sub> are almost the same values. On the other hand, at the transition state on the conrotatory pathway, the weights of the C<sub>3</sub>-C<sub>4</sub> and C<sub>5</sub>-C<sub>6</sub> are obviously larger than those of the C<sub>2</sub>-C<sub>3</sub>, C<sub>4</sub>-C<sub>5</sub>, and C<sub>6</sub>-C<sub>7</sub>. Thus, the relative relation for the weights of each  $\pi$  bond of benzene-ring at the disrotatory transition state is different from those at the conrotatory transition state. Therefore, the benzene ring of the disrotatory transition state shows much more aromatic nature than that of the conrotatory transition state, which corresponds to the small difference between the energy barriers of the conrotatory and disrotatory transition states.

#### 4. Conclusion

The potential energy surfaces for cyclic reactions of *o*-xylylene to benzocyclobutene were calculated by the ab initio CASSCF MO method. The transition state on the conrotatory pathway is 8.0 kcal/mol lower in energy than that on the disrotatory pathway. About half of the energy difference for both transition states comes from the orbital phase effects.

The six-membered ring part of *o*-xylylene shows the typical Kekulé structure (bonds alternation), and that of benzocyclobutene shows the aromatic structure. From the CiLC-IRC analysis, the bond exchange of the  $\pi$  bonds of C<sub>1</sub>-C<sub>2</sub> (and C<sub>7</sub>-

C<sub>8</sub>) and new  $\sigma$  bond of C<sub>1</sub>–C<sub>8</sub> occurs before the transition states, on the *o*-xylylene side, for both reaction pathways of the conrotatory and the disrotatory. For the disrotatory pathway, the bond exchange of the  $\pi$  bonds of C<sub>1</sub>–C<sub>2</sub> (and C<sub>7</sub>–C<sub>8</sub>) and the new  $\sigma$  bond of C<sub>1</sub>–C<sub>8</sub> occurs through the bi-radical character at the C<sub>1</sub> and C<sub>8</sub> atoms. At the transition state on the conrotatory pathway, the benzene ring part still has the nature of the Kekulé structure. On the other hand, the benzene ring part of the disrotatory transition state has the nature of the aromatic structure. The difference of the nature of the Kekulé and the aromatic structures for both transition states is the reason for the small difference between the activation energies of both reaction pathways.

**Acknowledgment.** The present research is supported by a Grant-in-Aid for Scientific Research from the Ministry of Education, Science and Culture of Japan. The computer time was made available by the Computer Center of the Institute for Molecular Science and by Osaka Sangyo University with its SGI Power Challenge computer.

## References and Notes

- (1) Houk, K. N.; Li, Y.; Evanseck, J. D. *Angew. Chem., Int. Ed. Engl.* **1992**, *31*, 682.
- (2) Houk, K. D.; Gonzalez, J.; Li, Y. *Acc. Chem. Res.* **1995**, *28*, 81.
- (3) Woodward, R. B.; Hoffmann, R. *The Conservation of Orbital Symmetry*, Verlag: Weinheim, Germany, 1970.
- (4) Fukui, K. *Acc. Chem. Res.* **1971**, *4*, 57.
- (5) Sakai, S. *J. Mol. Struct. (THEOCHEM)* **1999**, *461–462*, 283.
- (6) Sakai, S.; Takane, S. *J. Phys. Chem. A* **1999**, *103*, 2878.
- (7) Jefford, C. D.; Bernardinelli, G.; Wang, Y.; Spellmeyer, D. C.; Buda, A.; Houk, K. N. *J. Am. Chem. Soc.* **1992**, *114*, 4, 1157.
- (8) Roos, B. In *Advances in chemical physics*; Lawley, K. P., Ed.; Wiley: New York, 1987; Vol. 69, Part II, p 399.
- (9) Haviharan, P. C.; Polple, J. A. *Theor. Chim. Acta* **1973**, *28*, 213.
- (10) Gordon, M. S. *Chem. Phys. Lett.* **1980**, *76*, 163.
- (11) McDouall, J. J.; Peasley, K.; Roob, M. A. *Chem. Phys. Lett.* **1988**, *148*, 183.
- (12) Krishnan, R.; Binkley, J. S.; Seeger, R.; Pople, J. A. *J. Chem. Phys.* **1980**, *72*, 650.
- (13) Fukui, K. *J. Phys. Chem.* **1970**, *74*, 4161.
- (14) Ishida, K.; Morokuma, K.; Komornicki, A. *J. Chem. Phys.* **1977**, *66*, 2153.
- (15) Cundari, T. R.; Gordon, M. S. *J. Am. Chem. Soc.* **1991**, *113*, 5231.
- (16) Sakai, S. *J. Phys. Chem. A* **1997**, *101*, 1140.
- (17) Nguyen, T. R.; Chandra, A. K.; Sakai, S.; Morokuma, K. *J. Org. Chem.* **1999**, *64*, 65.
- (18) Sakai, S. *J. Phys. Chem. A* **2000**, *104*, 922.
- (19) Sakai, S. *Int. J. Quantum Chem.* **2000**, *80*, 1099.
- (20) Foster, J. M.; Boys, S. F. *Rev. Mod. Phys.* **1960**, *32*, 296, 300.
- (21) Bernardi, F.; Olivucci, M.; McDouall, J. J. W.; Robb, M. A. *J. Chem. Phys.* **1988**, *89*, 6365.
- (22) Bernardi, F.; Olivucci, M.; Robb, M. A. *Acc. Chem. Res.* **1990**, *23*, 405.
- (23) Formosinho, S.; Csizmadia, I. G.; Arnaut, L. G. *Theoretical and Computational Methods for Organic Chemistry*; Kluwer Academic Publisher: Norwell, MA, 1991, pp 289–313.
- (24) Schmidt, M. W.; Buldrige, K. K.; Boatz, J. A.; Jensen, J. H.; Koseki, S.; Gordon, M. S.; Nguyen, K. A.; Windus, T. L.; Elbert, S. T. *QCPE Bull.* **1990**, *10*, 52.
- (25) Frisch, K. J.; Trucks, G. W.; Schlegel, H. B.; Gill, P. M. W.; Johnson, B. G.; Robb, M. A.; Cheseman, J. R.; Keith, T. A.; Petersson, G. A.; Montgomery, J. A.; Raghavachari, K.; Al-Laham, M. A.; Zakrzewski, V. G.; Ortiz, J. V.; Foresman, J. B.; Cislowski, J.; Stefanov, B. B.; Nanayakkara, A.; Challacombe, M.; Peng, C. Y.; Ayala, P. Y.; Chen, W.; Wong, M. W.; Andres, J. L.; Replogle, E. S.; Comperts, R.; Martin, R. L.; Fox, D. J.; Binkley, J. S.; DeFrees, D. J.; Baker, J.; Stewart, J. P.; Head-Gordon, M.; Gonzalez, C.; Pople, J. A. *GAUSSIAN98*; Gaussian, Inc.: Pittsburgh, PA, 1998.
- (26) Miller, R. D.; Kolc, J.; Michl, J. *J. Am. Chem. Soc.* **1976**, *98*, 8510.
- (27) Flynn, C. R.; Michl, J. *J. Am. Chem. Soc.* **1974**, *96*, 3280.
- (28) Barton, J. W. *Ann. Rep. Prog.* **1970**, *70*, 405.
- (29) Tewson, T. J. *Ann. Rep. Prog.* **1974**, *71*, 299.
- (30) Dolbier, W. R., Jr.; McCullagh, D. R.; Robinson, D.; Anapolle, K. E. *J. Am. Chem. Soc.* **1975**, *97*, 934.
- (31) Migirdicyan, E.; Bandet, J. *J. Am. Chem. Soc.* **1975**, *97*, 7400.
- (32) Roth, W. R.; Biermann, M.; Dekker, H.; Jochems, R.; Mosselman, C.; Hermann, H. *Chem. Ber.* **1978**, *111*, 3892.
- (33) Roth, W. R.; Scholz, B. P. *Chem. Ber.* **1981**, *114*, 3741.
- (34) Munzel, N.; Schweig, A. *Angew. Chem., Int. Ed. Engl.* **1987**, *26*, 471.
- (35) The planarization of the structure could not rigorously separate the orbital and structural components of the barrier. In qualitative terms, however, we can understand the nature of the barrier.